Desalination and Water Treatment
www.deswater.com

doi: 10.5004/dwt.2019.23824

151 (2019) 372–383
May

Optimization of 4-chlorophenol regeneration from powdered activated carbon using response surface methodology

Tingting Zhang, Yanling Yang*, Xing Li, Nan Wang, Hang Li, Peng Du, Haikuan Yu, Siyang Ji, Zhiwei Zhou*

College of Architecture and Civil engineering, Beijing University of Technology, Beijing 100124, China, Tel. +86 10 67391726; emails: yangyanling@bjut.edu.cn (Y. Yang), hubeizhouzhiwei@163.com (Z. Zhou), zhangting1229ztt@163.com (T. Zhang), lixing@bjut.edu.cn (Xing Li), 15011163966@163.com (N. Wang), bjut_lihang@163.com (H. Li), 512742431@qq.com (P. Du), 41746250@qq.com (H. Yu), 489506654@qq.com (S. Ji)

Received 30 August 2018; Accepted 21 January 2019

ABSTRACT

In this study, an experimental study aimed at optimizing the factors affecting the regeneration amount of 4-chlorophenol (4-CP) from spent powdered activated carbon (PAC) is presented. For this response surface methodology (RSM) with Box-Behnken design was applied, which identified four variables (acoustic density, NaOH concentration, spent PAC dosage and ethanol concentration) in batch experiments. The physicochemical characteristics of the regenerated PAC under the optimal desorption condition was evaluated using thermogravimetric analysis, Fourier transform infrared spectroscopy (FTIR), Brunauer-Emmett-Teller (BET) and scanning electron microscopy, as compared with the virgin and spent PACs. Among the four variables, acoustic density and ethanol concentration (v/v, %) had stronger effect on the 4-CP desorption ($p < 0.001$). The predicted optimal 4-CP desorbing amount was 97.43 mg g^{-1}, and this matched well the observed performance of (96.94 ± 0.70) mg g^{-1}, obtained by acoustic density of 0.36 W mL^{-1}, NaOH concentration of 0.10 mol L^{-1}, spent PAC dosage of 0.93 g L^{-1} and ethanol concentration (v/v) of 24%. The result of thermogravimetric pyrolysis profiles of regenerated PAC confirmed that the adsorption behavior of 4-CP exhibited a chemisorption feature and desorption process was dominated by chemical reaction. Analysis of FTIR, pore structure and BET surface area demonstrated that ultrasound mainly acted on the surface functionalities, macro-pore and meso-pore structure of PAC. Additionally, the SEM images indicated that cavitation effect affected the surface roughness and surface cavities of PAC. The results here provided an insight into the application of ultrasound to regenerate saturated PAC with 4-CP.

Keywords: 4-chlorophenol; Desorption; Response surface methodology; Ultrasound; Optimization

1. Introduction

Aromatic compounds belong to a group of general environmental pollutants from industry. Phenolic derivatives are largely used as intermediates in the production of plastics, colors, pesticides, insecticides, etc. Many of them have been classified as hazardous pollutants because of their potential harm to human health. It has been well known that phenol, catechol and 2-chlorophenol can induce conformational changes in the human growth hormone [1]. Chlorophenols are considered as priority pollutants due to their toxic effects on organisms even at low concentrations. They cause distasteful taste and odor in drinking water, and can exert negative effects on different biological processes [2]. Chlorophenols are a large category of chemicals with chlorine atoms attached to the phenolic structure. The oil

* Corresponding authors.

1944-3994/1944-3986 © 2019 Desalination Publications. All rights reserved.

refining, textile, pesticide, as well as the pulp and paper industries have always produced high concentrations of phenols and chlorinated phenolic compounds in either their primary products, or their waste effluents [3]. Among the various chlorophenols, 4-chlorophenol (4-CP) is listed as one of the priority pollutants by the US Environmental Protection Agency and the European Union.

Activated carbon has been classified as one of the efficient adsorbents for removal of chlorophenols from wastewater because of its high surface area and unique chemical properties, i.e., polarity and nature of surface functional groups. The porous structure of activated carbon consists of a network of interconnected macro-pores, meso-pores, and micro-pores that provides a good capacity for the adsorption of organic molecules [4]. Adsorption by activated carbon has proved to be an efficient method for removing phenol and 4-CP [5–7]. Adsorption of phenolic compounds on activated carbon is easy to manage, however, the regeneration of activated carbon poses a major challenge because of the high affinity of the phenolic compounds to the activated carbon surface.

Over the years, a wide variety of regeneration techniques of activated carbon has been applied. The commonly used methods of thermal and chemical regeneration suffer the disadvantages of required high temperature and excessive burnout of activated carbon, pollution of the activated carbon by organic solvents or inorganic chemicals [8]. Other methods including biological [9], electrochemical [10], microwave irradiation [11], ultrasound assisted [12] and catalytic wet air oxidation regeneration [13] were also studied. An alternative method using ultrasound to regenerate adsorbents was also studied by some researchers [14,15]. The regeneration can transform the contaminants into less toxic byproducts, re-establish the adsorptive capacity of the activated carbon for the targeted chemicals, and increase its lifespan. Ultrasound is regarded as motivation force in chemical process to accelerate mass transfer following acoustic cavitation which emerged from growth and collapse of micrometrical bubbles and generation of final acoustic streaming induced by sonic waves [16]. Additionally, dissolved targeted compounds in the micrometer scale can form the bubble core during diffusion, and experience firsthand the effect of ultrasound through cavitation.

Response surface methodology (RSM) is a collection of mathematical and statistical techniques for modeling and analysis of problems in which a response of interest is influenced by several variables. This method is suitable for fitting a quadratic surface and it helps to optimize the effective parameters with a minimum number of experiments, as well as to analyze the interaction between the parameters. RSM are among the most popularly used methods to analyze adsorption experimental data. It provides an alternative for systems where the mathematical correlation between the parameters and the responses is unknown [17,18]. This method is composed of the process modeling step followed by estimation the optimal condition which subsequently construct first or second order polynomial equation for best prediction of real behavior of under study system over rotational space, following analysis of the variance (ANOVA). The validated model can be displayed in a tridimensional graph which introduce surface response useful for determination the optimal conditions [19]. It can also give information about dependency of response to each variable as function of their main effect and their interaction of other variables [20].

The main purpose of this study was to optimize the influence factors of ultrasound regeneration of 4-CP loaded onto powdered activated carbon (PAC) by using RSM. In addition, the regeneration mechanism of ultrasound was revealed by characterizing the regenerated PAC using thermogravimetric analysis (TGA), Fourier transform infrared spectroscopy (FTIR), Brunauer-Emmett-Teller (BET) and scanning electron microscopy (SEM), as compared with the fresh and spent PACs. The significance of the current study can provide an insight into the application of ultrasound to desorb of PAC saturated with phenolic pollutants.

2. Materials and methods

2.1. Materials and reagents

PAC (100 mesh) was obtained from Aladdin (Shanghai, China). The characteristics of the used PAC were as follows: iodine number 1,018.38 mg g^{-1}, methylene blue adsorption 230.74 mg g^{-1}, specific area 1,287 m^2 g^{-1}, average pore size 2.62 nm, micro-pore volume 0.25 cm^3 g^{-1}, meso-pore volume and macro-pore 0.57 cm^3 g^{-1} 4-CP (99%) and sodium hydroxide (≥98%) were purchased from Aladdin (Shanghai, China). Anhydrous ethanol was purchased from Sinopharm Chemical Reagent (Beijing, China). All chemicals used were analytical grade. All stock solutions were prepared using Milli-Q water (from a Millipore Milli-Q Ultrapure Gradient A10 purification system). Prior to use, PAC was washed and boiled for 3~4 times with Milli-Q deionized water. Afterwards, it was oven dried at 105°C to a constant weight and stored in a desiccator.

2.2. Adsorption experiments

The adsorption kinetic experiments were conducted at PAC dose of 1.0 g L^{-1} and the initial 4-CP concentration ranging from 50, 100, 150 to 200 mg L^{-1} at room temperature (25°C ± 2°C). Agitation of the solution was carried out with a mechanical stirrer at 300 rpm. The mixing lasted from 10 to 540 min. At designated time intervals, 5 mL samples were withdrawn and then filtered through a 0.45 μm cellulose acetate membrane. The concentration of 4-CP was calculated by the absorbance of the samples. Each experiment was carried out in triplicates.

Saturated PAC was prepared by adding 1.0 g of washed PAC to 1,000 mL of 100 mg L^{-1} 4-CP solution, stirring at 300 rpm for 2 d at room temperature (25°C ± 2°C) to ensure equilibrium was reached, before desorption experiments were conducted. The saturated PAC was dried at 90°C for 6 h, then weighted and kept in a desiccator for subsequent regeneration.

2.3. Desorption experiments using response surface methodology

Batch desorption experiments were carried out in an ultrasonic cleaner (YIU-3200DTS, Shanghai Yiyou Instruments Co., Ltd., China) with a maximum power output up to 180 W at fixed frequency of 40 kHz. A predetermined amount of 0.5, 1.0 and 1.5 g L^{-1} saturated PAC was introduced

into the sonoreactor, under the acoustic density of 0.18, 0.27 and 0.36 W mL^{-1} in the mixture of NaOH and EtOH. NaOH concentration varied at 0.05, 0.1 and 0.15 mol L^{-1}, and EtOH concentration changed from 10%, 20% to 30% (v/v).The temperature of the sonoreactor was not controlled and the reaction lasted for 210 min. All experiments were performed in triplicate and average findings were reported.

The Box-Behnken design (BBD), as the standard design of RSM, was used to optimize the experimental parameters. The dependent variables selected for this study were (i) X_1, acoustic density; (ii) X_2, NaOH concentration; (iii) X_3, saturated PAC mass; and (iv) X_4, ethanol concentration (v/v). The effect of the four variables and their interactions with each other were analyzed, and the values of variable levels are presented in Table 1. These were varied around the optimal values determined by single-factor experiments. The desorption capacity of PAC was dependent variable Y.

A polynomial quadratic equation was used for modeling of 4-CP desorption from PAC. Each response was used to develop an empirical model which correlated the response to the four regeneration variables using a second degree polynomial equation as given by the following Eq. (1) [21], where Y is the predicted response, b_0 is the constant coefficient, b_i is the linear coefficients, b_{ij} is the interaction coefficients, b_{ii} is the quadratic coefficients and x_i, x_j are the coded values of the PAC regeneration variables.

$$Y = b_0 + \sum_{i=1}^{n} b_i x_i + \left(\sum_{i=1}^{n} b_{ii} x_I^2\right) + \sum_{i=1}^{n-1} \sum_{j=i+1}^{n} b_{ij} x_i x_j \quad (1)$$

Design-Expert software version 10.3 (Stat-Ease, Inc., USA) and SAS software (SAS Institute) were used for the ANOVA and mathematical regression models were applied to determine the interaction between the independent variables and the response variable, and to plot response surfaces. ANOVA was used to determine the interaction between the processed variables and the response. Multiple regression analysis technique was used to evaluate the coefficient of the model. The quality of the model was examined with a correlation coefficient (R^2) and the F-test was used to check the statistical significance [22]. An error ratio for the model, based on expected output (Y_{exp}) and the observed output (Y_{obs}) from experiments was calculated as $(Y_{exp}-Y_{obs})/Y_{obs}$.

Of the 81 possible combinations, 27 including three replicates at the central point were tested, whose settings are summarized in Table 2. The order in which experiments were performed was mingled to avoid influencing the outcomes.

Table 1
Experimental values and coded levels of the independent variables used for BBD

Symbol	Independent variables	Level		
		–1	0	+1
X_1	Acoustic density (W mL^{-1})	0.18	0.27	0.36
X_2	NaOH concentration (mol L^{-1})	0.05	0.1	0.15
X_3	Saturated PAC mass (g L^{-1})	0.5	1.0	1.5
X_4	Ethanol concentration (v/v, %)	10	20	30

2.4. Analytical methods

The concentration of 4-CP was monitored by UV–vis spectrophotometric (UV-2600, SOPTOP, China) at wavelength of 279 nm. The FTIR (V70/HYPERION 1000, Bruker, USA) was applied to qualitatively identify the chemical functional groups. The wavenumber range was 4,000~400 cm^{-1}. The surface physical morphology of the PAC was observed using a scanning electron microscopy (JEM 2100F, JEOL, Japan). The BET specific surface area (S_{BET}) and Barrett-Joyner-Halenda (BJH) pore size distribution of the PACs were investigated by applying N_2 adsorption-desorption isotherm analysis carried out at 77 K (TRISTAR II 3020M, Micromeritics, USA). The PAC samples were degassed under vacuum at 150°C for 3 h prior to analysis. Thermogravimetry analysis was carried out using high temperature TGA/DSC synchronous thermal analyzer (TGA/DSC 1, METTLER-TOLEDO, Switzerland). For each measurement, about 4.0 mg PAC sample was placed under argon atmosphere (50.0 mL min^{-1}) and heated from 30°C to 800°C with the rate of 10 K min^{-1}.

The amount of 4-CP absorbed at equilibrium q_e (mg g^{-1}) was calculated by the following Eq. (2), the absolute desorbed amount q_d (mg g^{-1}) of 4-CP after regeneration was calculated using Eq. (3).

$$q_e = \frac{(c_0 - c_e)V}{w} \quad (2)$$

$$q_d = \frac{c_d V}{m} \quad (3)$$

where C_0 and C_e are the initial and equilibrium concentrations of 4-CP (mg L^{-1}), C_d is the concentration of 4-CP in desorption solution. V is the adsorption/desorption liquid volume (L), w is the weight of dried adsorbent used (g) and m is the saturated carbon dosage (g), respectively.

3. Results and discussion

3.1. Adsorption characteristics of 4-CP

The adsorption kinetics shown that 4-CP adsorption approached equilibrium at 540 min for different concentrations (50, 100, 150 and 200 mg L^{-1}), and the experimentally obtained q_e of the four predetermined concentrations were 47.72, 96.81, 141.47 and 173.29 mg g^{-1}, respectively.

Adsorption kinetics studies were carried out to determine the potential rate controlling steps involved in the mechanism of solute adsorption onto the adsorbent. In this study, the pseudo-first-order, pseudo-second-order and intra-particle diffusion models were applied. The pseudo-first-order model is based on the membrane diffusion theory, and it assumes the external diffusion is the determining step in the adsorption process. The pseudo-second-order model is based on the rate control steps of chemical reactions or through electron sharing or electron gain and loss of chemical adsorption. The intra-particle model assumes that the intra-particle

Table 2
Box-Behnken design and experimental data

Experimental run	Influence factor X				Y, Desorption amount (mg g^{-1})		Error $(Y_{exp}-Y_{obs})/Y_{obs}$ [a]100%
	Acoustic density (W mL^{-1}) X_1	NaOH concentration (mol L^{-1}) X_2	Saturated PAC mass (g L^{-1}) X_3	Ethanol concentration (v/v, %) X_4	Observed (Y_{obs})	Expected (Y_{exp})	
1	0.36	0.1	1	30	97.38	101.61	4.34
2	0.18	0.1	1	10	64.35	64.71	0.56
3	0.27	0.1	1	20	86.80	86.79	–0.01
4	0.27	0.1	1	20	86.80	86.79	–0.01
5	0.27	0.15	1	30	83.99	85.54	1.85
6	0.36	0.15	1	20	87.18	81.42	–6.61
7	0.27	0.1	1.5	30	96.88	92.11	–4.92
8	0.27	0.05	1	30	77.55	76.41	–1.47
9	0.27	0.15	0.5	20	64.44	65.50	1.64
10	0.27	0.05	1.5	20	65.00	68.53	5.43
11	0.36	0.1	0.5	20	86.62	87.55	1.07
12	0.27	0.05	1	10	59.44	59.81	0.62
13	0.27	0.1	0.5	30	83.31	81.29	–2.42
14	0.18	0.05	1	20	64.22	63.48	–1.15
15	0.27	0.1	1.5	10	69.85	65.36	–6.43
16	0.18	0.1	1.5	20	78.44	79.42	1.25
19	0.18	0.1	1	30	84.76	86.90	2.52
18	0.27	0.1	1	20	86.80	86.79	-0.01
19	0.27	0.05	0.5	20	62.65	63.13	0.77
20	0.36	0.1	1.5	20	87.96	88.60	0.73
21	0.36	0.05	1	20	85.77	83.29	–2.89
22	0.27	0.1	0.5	10	65.08	63.34	–2.67
23	0.18	0.1	0.5	20	66.35	67.63	1.93
24	0.36	0.1	1	10	76.66	79.10	3.18
25	0.27	0.15	1.5	20	68.83	72.94	5.97
26	0.27	0.15	1	10	54.41	57.46	5.61
27	0.18	0.15	1	20	76.15	72.13	–5.28

[a]Experiments 3, 4, and 18 were replicates experiments.

diffusion step is the rate-limiting one. The intercept of the plot indicated the effect of external mass transfer: the larger the intercept, the greater the contribution of external mass transfer in the rate-limiting step. The rate constants and correlation coefficients corresponding to the three models are listed in Table 3.

As observed in Table 3, the adsorption capacity (q_e) obtained at equilibrium experimentally was not consistent with the pseudo-first-order kinetic model. The R^2 value was unsatisfactory, which implied that the pseudo-first-order model was not clearly to explain the experimental result. While, in case of pseudo-second-order model, the experimental

and calculated values for q_e were relatively similar and the R^2 value were closer to 1. For intra-particle diffusion model, the intercepts do not pass through the origin indicated that the intra-particle diffusion was not the sole rate controlling step for 4-CP adsorption on PAC. Moreover, C represents boundary layer effect, which indicated that a greater value of C responded to a larger boundary layer thickness [23]. Thus, the pseudo-second-order model performed better than the other two model to describe the adsorption of 4-CP onto PAC, which indicated that chemisorption governed the adsorption process.

3.2. Response surface methodological approach

3.2.1. Model development and statistical analysis

Analysis of variance (ANOVA) was carried out to justify the adequacy of the model. The ANOVA for the quadratic model is depicted in Table 4. The predictive values of the model were demonstrated by a coefficient of variation (CV) of 5.09% and a predicted residual error sum of squares (PRESS) of 1,050.27, a correlation coefficient R^2 of 0.9502 with Adj. R^2 of 0.892, and a Pred. R^2 of 0.713, and an adequate precision (AP) of 15.196. All criteria defined

Table 3
Adsorption kinetics parameters of 4-CP onto PAC

Models	Pseudo-first-order			Pseudo-second-order			Intra-particle diffusion		
Equations	$\lg(q_e - q_t) = \lg q_e - \frac{k_1}{2.303}t$			$\frac{t}{q_t} = \frac{1}{k_2 q_e^2} + \frac{t}{q_e}$			$q_t = K_{id} t^{\frac{1}{2}} + C$		
C_0 (mg L^{-1})	k_1	q_e	R^2	k_2	q_e	R^2	K_{id}	C	R^2
50	0.0067	0.51	0.942	0.0431	46.92	**0.999**	0.03023	47.2348	0.891
100	0.0061	1.32	0.885	0.0150	96.74	**0.999**	0.09018	93.4316	0.702
150	0.0037	4.63	0.911	0.0041	142.56	**0.999**	0.23125	133.787	0.881
200	0.0066	12.97	0.978	0.0014	174.21	**0.999**	0.62356	149.151	0.923

Note: The correlation coefficient R^2 values >0.995 are shown in bold.

Table 4
Regression coefficients and statistical parameters describing the effect of the independent variables

Subject	Quadratic sum	Freedom	Mean square	F-value	Significance (p)
Model	3,479.57	14	248.54	16.36	<0.0001
X_1	635.18	1	635.18	41.8	<0.0001
X_2	34.47	1	34.47	2.27	0.1579
X_3	123.58	1	123.58	8.13	0.0146
X_4	1,498.15	1	1,498.15	98.6	<0.0001
X_1X_2	27.67	1	27.67	1.82	0.2021
X_1X_3	28.91	1	28.91	1.9	0.1929
X_1X_4	0.025	1	0.025	1.67×10^{-3}	0.9681
X_2X_3	1.04	1	1.04	0.068	0.798
X_2X_4	32.93	1	32.93	2.17	0.1667
X_3X_4	19.35	1	19.35	1.27	0.2811
X_1^2	3.24	1	3.24	0.21	0.6526
X_2^2	832.74	1	832.74	54.8	<0.0001
X_3^2	244.74	1	244.74	16.11	0.0017
X_4^2	107.71	1	107.71	7.09	0.0207
Residual	182.34	12	15.19		
Lack of Fit	182.34	10	18.23		
Pure Error	0.000	2	0.00		
Cor Total	3,661.91	26			

Note: $p \leq 0.0001$: highly significant; $p \leq 0.001$: strongly significant; $p \leq 0.05$: significant; $p > 0.05$: not significant.

by Montgomery that a model should meet to be properly fitting were fulfilled: missing items *F*-value > 0.1; R^2 > 0.95; Adj. R^2-Pred. R^2 <0.2; CV <10%; Pred. R^2> 0.7; AP > 4 [24]. The quadratic model was therefore considered suitable for prediction.

As seen in Table 4, the model was considered to be statistically significant because the associated Prob. > *F* value for the model was lower than 0.05 (i.e. a = 0.05, or 95% confidence), in other words an F-value of 16.36 and p < 0.0001 confirmed that the model was highly significant, as were the variables X_1, X_4 and X_2^2. For the model terms, Prob > *F* less than 0.05 indicated that the model terms were significant. In this case, the parameters X_3, X_3^2 and X_4^2 were significant. In contrast, the parameter X_2 was not significant (p > 0.05) to the response. The results shown that it was feasible to use the regression model to predict the optimum conditions for the regeneration of the PAC saturated with 4-CP. From the level of significance of the regression coefficients (Table 4), it was concluded that in the model the most influential single factor for PAC regeneration *Y* was ethanol concentration (X_4), followed by acoustic density (X_1), saturated PAC mass (X_3) and NaOH concentration (X_2). Moreover, from the statistical results obtained, it indicated that the above model was adequate to predict the desorption amount of 4-CP. As seen, the predicted values obtained were quite close to the experimental values (seen in Fig. 1), indicating that the model developed was successful in capturing the correlation between the regeneration variables to the response.

A polynomial regression equation was developed to analyze the factor interactions by identifying the significant factors contributing to the regression model. An empirical relationship between the response (*Y*) and the independent variables was expressed by the following Eq. (4).

$$Y = 86.79 + 7.28X_1 + 1.69X_2 + 3.21X_3 + 11.17X_4 - 2.63X_1X_2 - 2.69X_1X_3 + 0.08X_1X_4 + 0.51X_2X_3 + 2.87X_2X_4 + 2.20X_3X_4 + 0.78X_1^2 - 12.50X_2^2 - 6.77X_3^2 - 4.49X_4^2 \quad (4)$$

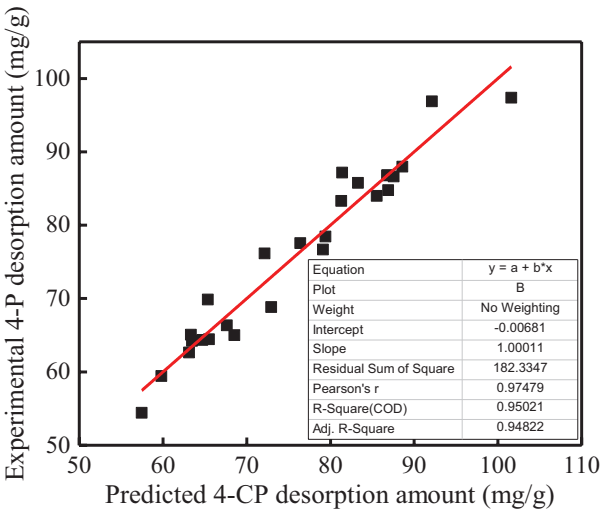

Fig. 1. Predicted vs. experimental 4-CP desorbed amount.

3.2.2. Interaction of variables

The interactive effects of the independent variables on the dependent variable were illustrated by three- and two-dimensional contour plots (Fig. 2), according to the suggested fitted model. Both types of plots showed the effects of two out of the four independent variables on the response factor.

As seen in Fig. 2(a), the desorption amount increased with the increase of acoustic density (X_1). While in case of the NaOH concentration (X_2), the desorption amount first increased and then decreased, with an optimum at 0.10 mol L^{-1}. Furthermore, acoustic density and NaOH interacted with each other as this combination produced an elliptic profile. It is evident from the elliptical nature of the contours that the interaction between the individual variables was significant [25].The increase in desorption amount with increase of acoustic density could be explained by cavitation effects on the solid-liquid interface.

Fig. 2(b) displays that the 4-CP desorption amount decreased with an increase of saturated PAC dosage (X_3), with an optimum saturated PAC mass at 0.93 g L^{-1}. Fig. 2(b) shows an elliptical curve with a strong interaction between the two parameters. The graph displayed that the maximum desorption (97.43 mg g^{-1}) occurred under high acoustic density, at spent PAC dose of 0.93 g L^{-1}, which was in accordance with the model. Increasing the spent PAC dosage could decline the concentration gradient between solute concentrations and the adsorbent surface. Moreover, the higher amounts of saturated PAC could lead to the decreased surface area of PAC, and the unavailability of adsorption sites, as well as the competition with target contaminants for adsorption sites [12].

Fig. 2(c) represents the interaction between acoustic density (X_1) and ethanol concentration (X_4), again producing an elliptical curve with strong interaction between the two parameters. As shown in Fig. 2(c), the 4-CP desorption amount generally increased with increase of acoustic density and ethanol concentration. Higher acoustic density and ethanol concentration were favorable for enhancing the 4-CP desorption amount as the increased ethanol concentration would reduce the tensile stress of the mixture, and lower the cavitation threshold, thus leading to the increase cavitation effect of the ultrasound process.

It can be found from Fig. 2(d) that the plots were approximately symmetrical in shape with circular contours. The circular nature of the contour signified that the interactive effects between the variables were not significant, a weak interaction existed between two variables of NaOH concentration (X_2) and saturated PAC mass (X_3), and the optimum values of the test variables could not be easily obtained.

Fig. 2(e) illustrates the interaction effect of NaOH concentration (X_2) and ethanol concentration (X_4) on the desorption amount. As observed, the desorption amount increased with increase of ethanol concentration (X_4), while the desorption amount of 4-CP decreased with an increase in NaOH concentration (X_2). Ethanol could facilitate the generation of bubbles and capture primary radicals (•OH) to form secondary radicals of $\bullet C_2H_4OH$ and accelerate the reaction rate. The decreased desorption amount by NaOH

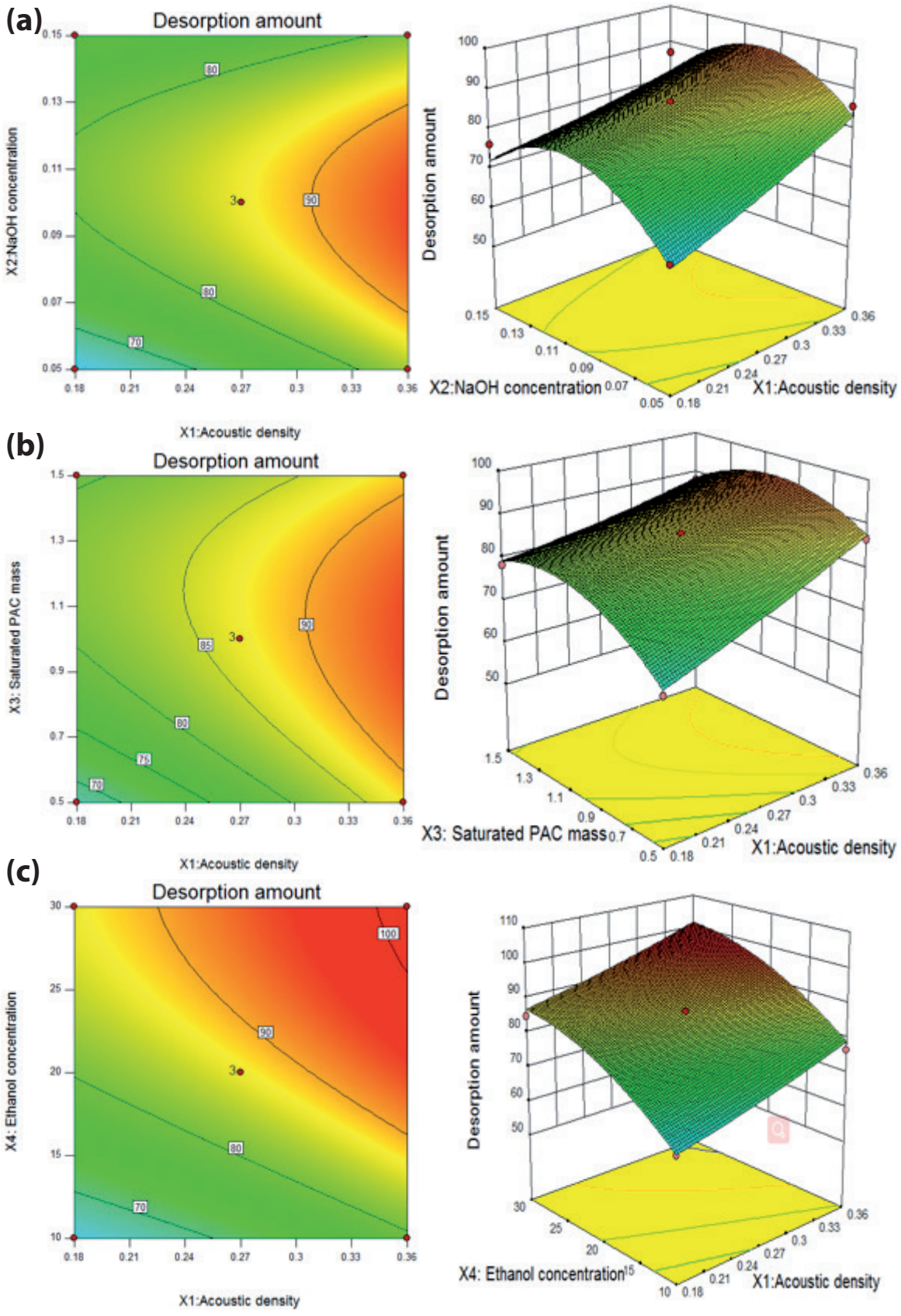

Fig. 2. (*Continued*)

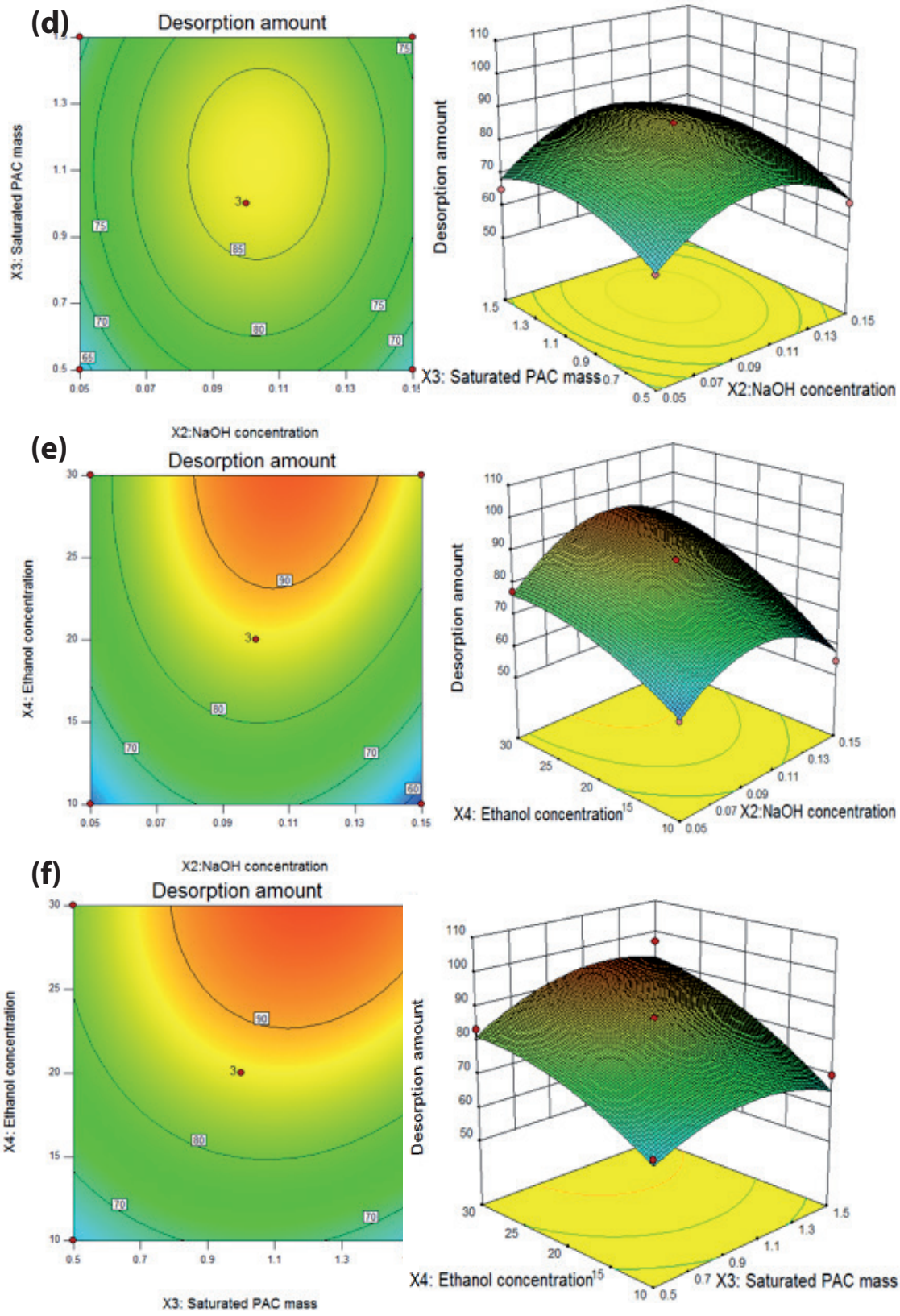

Fig. 2. Contour plots showing the interdependence of two variables and 4-CP desorption amount with a 2-D representation (left) and a 3-D representation (right) for each set. (a): acoustic density X_1 and NaOH concentration X_2. (b): acoustic density X_1 and saturated PAC mass X_3. (c): acoustic density X_1 and ethanol concentration X_4. (d): NaOH concentration X_2 and saturated PAC mass X_3. (e): NaOH concentration X_2 and ethanol concentration X_4. (f): saturated PAC mass X_3 and ethanol concentration X_4.

could be explained by the following aspects: first, a higher NaOH concentration could increase the ionization of 4-CP. The ionization of 4-CP decreased when pH surpassed 12, thereby the desorption capacity decreased. The phenomenon was also observed by Hamdaoui and Naffrechoux [26]; Second, negative charge increased on the PAC surface in the increased concentration of NaOH.

As observed in Fig. 2(f), a weak interaction with a clear optimum was observed for saturated PAC mass (X_3) in comparison with ethanol concentration (X_4). The desorption amount was found to decrease with increase of saturated PAC dosage, and increased with the increase of ethanol concentration. An increase in saturated PAC dosage decreased the adsorption sites, which could also decrease the concentration gradient, thereby resulting in decreasing desorption amount. Moreover, ethanol is a weak polarity solvent which could be benefit for desorption of 4-CP from PAC.

3.2.3. Model validation

By partial differentiation of the established second-order regression model, the optimum conditions for maximum 4-CP desorption amount was obtained, with acoustic density of 0.36 W mL^{-1}, NaOH concentration of 0.10 mol L^{-1}, spent PAC dosage of 0.93 g L^{-1} and ethanol concentration of 24% (v/v). Under these conditions, the second-order model predicted a maximum desorption amount of 97.43 mg g^{-1}. Three groups of parallel tests were carried out to verify the predicted maximal desorption amount. It was observed that the experimental values of (96.94 ± 0.70) mg g^{-1} were obtained, which were in good agreement with the values predicted from the models, with small error of 1.09% between the predicted and the actual values.

3.3. Thermogravimetric analysis

The thermal gravimetric analysis (TGA) and derivative thermogravity (DTG) of regenerated PAC under the optimal condition, in contrast to the fresh and spent PAC are depicted in Fig. 3.

As indicated in Fig. 3, the TGA and DTG curves of fresh PAC displayed a small weight loss (about 12.7%) in the entire temperature range, most likely due to the removal of adsorbed water and surface oxygen groups. In the DTG curve of spent PAC sample, the peak centered at 234°C was assigned to the physisorbed fraction. Beyond 234°C, a broad decline region of 234~591°C was observed, which was related to a typical chemisorption.

As seen in Table 5, for regenerated PAC, at temperature from 35°C to 107°C, a gradual reduction occurred due to the removal of the water molecules including the fracture of hydrogen bond among H_2O. The relative low mass loss of 234°C~591°C was attributed to the phenols physical desorption [27]. The high mass loss (49.6%) centered at 591°C~800°C corresponding to the presence of physisorbed and chemisorbed of 4-CP was observed, which was attributed to the decomposition of 4-CP molecules including the intermediates of carbonized phenolic residues and cleavage of chemical bonding on the PAC surface. Such high mass loss (49.6%) at 591°C~800°C of regenerated PAC was closed to seven times higher than that of the spent PAC (7.6%). Moreover, this result implied that the intermediate products

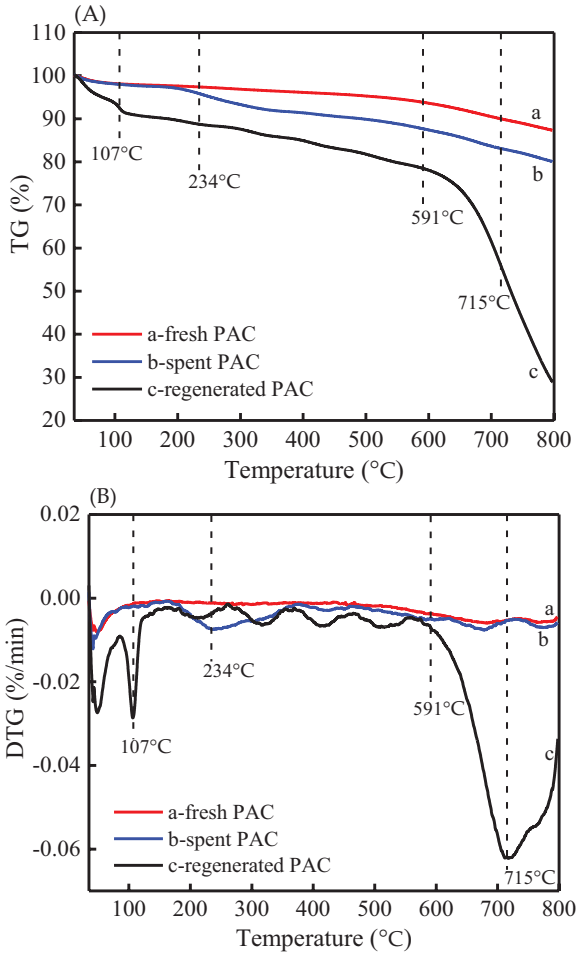

Fig. 3. (A) Thermal gravimetric analysis (TG) and (B) derivative thermogravity (DTG) curves of three PAC samples (a) fresh; (b) spent; and (c) regenerated.

Table 5
Weight losses of different PAC during the thermal heating process

PAC type	Weight loss at different temperature range (%)				Total weight loss (%)
	35°C~107°C	107°C–234°C	234°C–591°C	591°C–800°C	35°C~800°C
Fresh	1.9	0.7	3.6	6.5	12.7
Spent	2.0	2.1	8.2	7.6	19.9
Regenerated	7.5	3.8	10.2	49.6	71.1

or small molecules were more easily to be degraded than 4-CP molecule itself. The peak at temperature around 591°C (in Fig. 3 DTG curve) was presumably related to the decomposition of surface functionalities. Therefore, adsorption of 4-CP exhibited a chemisorption feature, which suggested that the forces involved in this process were mainly dominated by chemical reactions. Additionally, there was a continuous decrease in mass fraction when the temperature surpassed 715°C. This stage was related to thermal carbonization processes of intermediates or small molecules.

3.4. FTIR analysis

Fig. 4 depicts FTIR spectra of fresh, spent and regenerated PACs. According to Fig. 4, all PAC samples spectrum displayed a band of stretching –OH vibrations (3,600–3,000 cm^{-1}) due to the carbon surface hydroxyl groups and chemisorbed water [28]. As for fresh PAC, the vibration around 1,587 cm^{-1} was assigned to the aromatic C=C stretching, and the peak near 1,206 cm^{-1} was related to the stretching vibrations of C–O. The presence of a band at 2,850 cm^{-1} was attributed to the stretching vibrations of C–H.

The spectra of regenerated PAC displayed an absorption peak at around 3,720 cm^{-1} that was assigned to stretching vibrations of –OH in phenols structural environments. The characteristic absorption peak at 1,587 and 1,206 cm^{-1} was related to the stretching vibrations of C=C in benzene ring and C–O in carboxylic acid, respectively. Additionally, the obvious absorption peak at around 820 cm^{-1} was ascribed to the Ar-H out-of-plane bending in phenyl. For spent PAC, the spectra presented another two peaks at 1,429 and 878 cm^{-1}, which were corresponded to the skeleton vibration of C=C and the para-position substituent groups on the benzene ring. The peak near 692 cm^{-1} was assigned to the stretching vibrations of C–Cl.

Comparing with the spectra of the spent PAC with regenerated PAC, it is noted that the absorption peaks at 1,429, 1,206, 820 and 692 cm^{-1} clearly decreased, which were related to the functional groups of C=C, C–O, Ar-H and C–Cl. This was due to the interruption of some chemical bonds and removal of superficial groups. The presence of the hydroxyl radicals produced in ultrasound process would play an important role in this phenomenon. Hydroxyl radicals might react with the functional groups on the spent PAC surface, leading to an increase in desorption capacity. The results would suggest that the free radicals oxidation effect was one of the attributions for efficient regeneration of PAC.

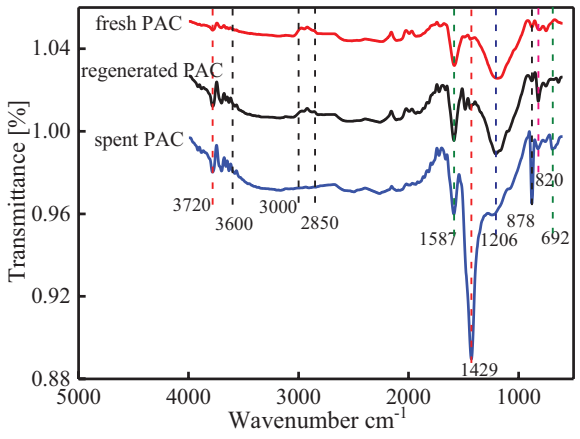

Fig. 4. FTIR spectra of fresh spent and regenerated PAC samples.

3.5. Specific surface area and pore structural analysis

The surface area and the pore structure of the PACs were studied by performing N_2 physical adsorption-desorption studies. According to the classification of IUPAC pore dimensions, the pores of adsorbents can be classified into micro-pore (d < 2 nm), meso-pore (d = 2~50 nm) and macro-pore (d > 50 nm). The nitrogen adsorption-desorption isotherms of the three PACs are illustrated in Fig. 5. The shapes of their N_2 adsorption-desorption isotherms were fitted with types IV according to the IUPAC classification, with a wider hysteresis loop at high relative pressures, implied that PACs possessed a mixed structure of microporous and mesoporous.

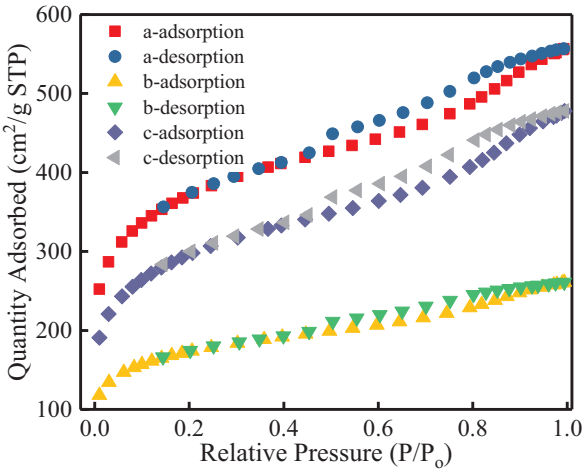

Fig. 5. N_2 adsorption isotherm of the three types of PAC (a) fresh; (b) spent; and (c) regenerated.

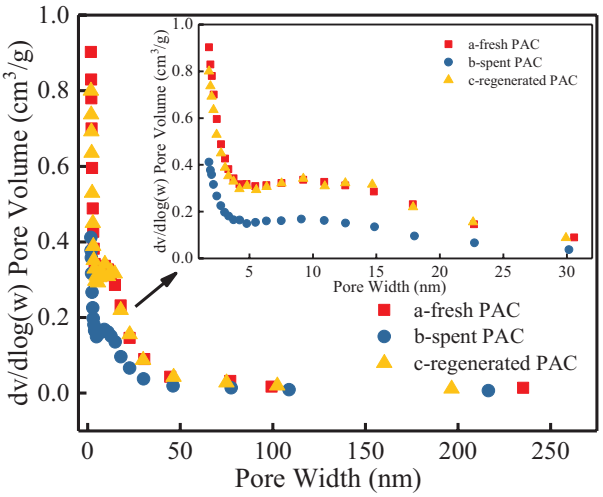

Fig. 6. Pore size distribution obtained from nitrogen adsorption isotherms for three types of PAC (a) fresh; (b) spent; and (c) regenerated.

Table 6
Textual properties of the three PAC samples

PAC type	Specific surface area (m^2g^{-1})			Pore volume ($cm^3\ g^{-1}$)			Pore diameter (nm) Average pore size
	BET surface area	t-Plot external surface area	t-Plot micro-pore area	Total pore volume	t-Plot micro-pore volume	Meso-pore and macro-pore volume	
Fresh	1,287.59	747.33	540.26	0.82	0.25	0.57	2.62
Spent	603.99	353.58	250.42	0.40	0.11	0.29	2.64
Regenerated	1,043.91	696.11	347.80	0.71	0.15	0.56	2.79

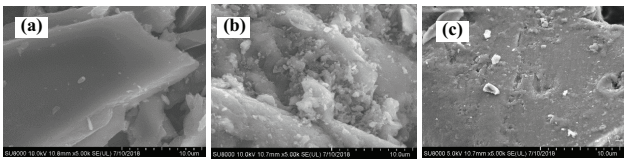

Fig. 7. SEM images of the three PAC samples (a) fresh; (b) spent; and (c) regenerated (Magnification 5000).

The pore size distribution and the corresponding parameters are displayed in Fig. 6 and summarized in Table 6. As shown in Fig. 6 that a majority of the pores fell into the rage of meso-pore (between 2 and 10 nm). The specific surface area (S_{BET}) of the fresh PAC was found to be 1,287.59 $m^2\ g^{-1}$, with the proportion of micro-pore area reached 42%. When saturated with 4-CP, the S_{BET} and total volume significantly decreased. However, it is obvious that the S_{BET} and total volume increased by 72.8% and 77.5%, after the spent PAC subjected to ultrasonic, respectively. Additionally, the meso-pore and macro-pore volume were enlarged for regenerated PAC, and the meso-pore and macro-pore volume increased by 78.8% of the total volume, and the average pore diameter increased after ultrasonic regeneration. These results indicated that ultrasound could expand the meso-pore and macro-pore of PAC.

The morphologies of three PAC samples were shown in Fig. 7. The fresh PAC exhibited a flat surface without any palpable pore (Fig. 7(a)). Small aggregates of contaminants adhered on the surface of the spent PAC (Fig. 7(b)). After suffered from ultrasonic treatment, significant small cavities appeared on the surface of the PAC and the PAC topography was rough. Additionally, the amount of contaminants on the surface was obviously reduced (Fig. 7(c)).

4. Conclusion

The desorption of 4-CP from saturated PAC in the presence of ultrasound was investigated, focusing on optimizing influence parameters such as acoustic density, NaOH concentration, saturated PAC mass and ethanol concentration by RSM. The main conclusions of this work were as following:

1. The adsorption kinetics of 4-CP fitted well with pseudo-second-order model, and chemisorption governed the adsorption process.
2. Among the four variables, acoustic density and ethanol concentration (v/v) had stronger effect on the 4-CP desorption ($p < 0.001$). A good correlation between the experimental and predicted values was obtained, showing that the response models were accurate and adequate to represent the process behavior. The optimum regeneration conditions were as follows: 0.36 W mL^{-1} of acoustic density, 0.1 mol L^{-1} of NaOH concentration, 0.93 g L^{-1} of spent PAC mass and 24% (v/v) of ethanol concentration. The optimum maximum desorption amount of 97.43 mg g^{-1} was obtained.
3. Analysis of FTIR, pore structure and BET surface area demonstrated that ultrasound mainly acted on the surface functionalities, macro-pore and meso-pore structure of PAC. SEM results showed that the surface of the PAC becomes rough after ultrasound regeneration.

Acknowledgements

The authors acknowledge the financial support of the National Natural Science Foundation of China (51778012). We would like to give our sincere thanks to the peer-reviews for their suggestions.

References

[1] Y.F. Maa, C.C. Hsu, Aggregation of recombinant human growth hormone induced by phenolic compounds, Int. J. Pharm., 140 (1996) 155–168.
[2] B.H. Hameed, L.H. Chin, S. Rengaraj, Adsorption of 4-chlorophenol onto activated carbon prepared from rattan sawdust, Desalination, 225 (2008) 185–198.
[3] M.F. Sze, G. McKay, Enhanced mitigation of para-chlorophenol using stratified activated carbon adsorption columns, Water. Res., 46 (2012) 700–710.
[4] H. Allaboun, F.A.A. Al-Rub, Removal of 4-Chlorophenol from contaminated water using activated carbon from dried date pits: equilibrium, kinetics, and thermodynamics analyses, Materials, 9 (2016) 251–266.
[5] K. Pirzadeh, A.A. Ghoreyshi, Phenol removal from aqueous phase by adsorption on activated carbon prepared from paper mill sludge, Desal. Wat. Treat., 52 (2014) 6505–6518.
[6] Q. Zhao, H.J. Han, S.Y. Jia, H.F. Zhuang, B.L. Hou, F. Fang, Adsorption and bioregeneration in the treatment of phenol, indole, and mixture with activated carbon, Desal. Wat. Treat., 55 (2015) 1876–1884.
[7] M.S. Bilgili, G. Varank, E. Sekman, S. Top, D. Özçimen, R. Yazıcı, Modeling 4-chlorophenol removal from aqueous solutions by granular activated carbon, Environ. Model. Assess., 17 (2012) 289–300.
[8] O. Korkut, E. Sayan, O. Lacin, B. Bayrak, Investigation of adsorption and ultrasound assisted desorption of lead (II) and copper (II) on local bentonite: a modelling study, Desalination, 259 (2010) 243–248.
[9] M.E. Gamal, H.A. Mousa, M.H. El-Naas, R.j. Zachariac, S. Judd, Bio-regeneration of activated carbon: a comprehensive review, Sep. Purif. Technol., 197 (2018) 345–359.

[10] L.Z. Wang, N. Balasubramanian, Electrochemical regeneration of granular activated carbon saturated with organic compounds, Chem. Eng. J., 155 (2009) 763–768.
[11] E. Yagmur, S. Turkoglu, A. Banford, Z. Aktas, The relative performance of microwave regenerated activated carbons on the removal of phenolic pollutants, J. Cleaner. Prod., 149 (2017) 1109–1117.
[12] S. Guilane, O. Hamdaoui, Ultrasound-assisted regeneration of granular activated carbon saturated by 4-chlorophenol in batch-loop reactor, Desal. Wat. Treat., 57 (2016) 17262–17270.
[13] I. Benhamed, L. Barthe, R. Kessas, C. Julcour, H. Delmas, Effect of transition metal impregnation on oxidative regeneration of activated carbon by catalytic wet air oxidation, Appl. Catal. B., 187 (2016) 228–237.
[14] G. Jing, Z. Zhou, S. Lei, M. Dong, Ultrasound enhanced adsorption and desorption of chromium (VI) on activated carbon and polymeric resin, Desalination, 279 (2011) 423–427.
[15] Z.H. Sun, C. Liu, Z. Cao, W. Chen, Study on regeneration effect and mechanism of high-frequency ultrasound on biological activated carbon, Ultrason. Sonochem., 44 (2018) 86–96.
[16] M.S. Tehrani, R. Zare-Dorabei, Highly efficient simultaneous ultrasonic-assisted adsorption of methylene blue and rhodamine B onto metal organic framework MIL-68(Al): central composite design optimization, RSC. Adv., 6 (2016) 27416–27425.
[17] S. Hajati, M. Ghaedi, Z. Mahmoudi, R. Sahraei, SnO_2 nanoparticle-loaded activated carbon for simultaneous removal of Acid Yellow 41 and Sunset Yellow; derivative spectrophotometric, artificial neural network and optimization approach, Spectrochim. Acta., Part A., 150 (2015) 1002–1012.
[18] A. Asfaram, M. Ghaedi, M.H.A. Azqhandi, A. Goudarzi, M. Dastkhoon, Statistical experimental design, least squares-support vector machine (LS-SVM) and artificial neural network (ANN) methods for modeling the facilitated adsorption of methylene blue dye, RSC. Adv., 6 (2016) 40502–40516.
[19] E.A. Dil, M. Ghaedi, G.R. Ghezelbash, A. Asfaram, M.K. Purkait, Highly efficient simultaneous biosorption of Hg^{2+}, Pb^{2+} and Cu^{2+} by Live yeast Yarrowia lipolytica 70562 following response surface methodology optimization: kinetic and isotherm study, J. Ind. Eng. Chem., 48 (2017) 162–172.
[20] G.R. Bardajee, S. Azimi, M.B.A.S. Sharifi, Application of central composite design for methyl red dispersive solid phase extraction based on silver nanocomposite hydrogel: microwave assisted synthesis, Microchem. J., 133 (2017) 358–369.
[21] N.F. Zainudin, K.T. Lee, A.H. Kamaruddin, S. Bhatia, A.R. Mohamed, Study of adsorbent prepared from oil palm ash (OPA) for flue gas desulfurization, Sep. Purif. Technol., 45 (2005) 50–60.
[22] M. Alimohammady, M. Jahangiri, F. Kiani, H. Tahermansouri, Highly efficient simultaneous adsorption of Cd (II), Hg (II) and As (III) ions from aqueous solutions by modification of graphene oxide with 3-aminopyrazole: central composite design optimization, New J. Chem., 41 (2017) 8905–8919.
[23] C.K. Lee, K.S. Low, P.Y. Gan, Removal of some organic dyes by acid treated spent bleaching earth, Environ. Technol., 20 (1999) 99–104.
[24] D. C Montgomery, Design and Analysis of Experiments, 6th ed., Wiley & Sons, New York, 2009.
[25] M. Rajasimman, P. Karthic, Application of response surface methodology for the extraction of chromium (VI) by emulsion liquid membrane, J. Taiwan. Inst. Chem. Eng., 41 (2010) 105–110.
[26] O. Hamdaoui, E. Naffrechoux, Modeling of adsorption isotherms of phenol and chlorophenols onto granular activated carbon: Part I. Two-parameter models and equations allowing determination of thermodynamic parameters, J. Hazard Mater., 147 (2007) 381–394.
[27] M.Y. Cheng, S.C. Yang, C.T. Hsieh, Thermal regeneration of activated carbons exhausted with phenol compound, Sep. Purif. Technol., 42 (2007) 639–652.
[28] J.A. Banuelos, O. Garcia-Rodriguez, F.J. Rodriguez-Valadez, J. Manriquez, E. Bustos, A. Rodriguez, L.A. Godinez, Cathodic polarization effect on the electro-Fenton regeneration of activated carbon, J. Appl. Electrochem., 45 (2015) 523–531.